

Energy transport by lattice solitons in α -helical proteins

D. Hochstrasser, F. G. Mertens, and H. Büttner

Physics Institute, University of Bayreuth, D-8580 Bayreuth, Federal Republic of Germany

(Received 28 March 1989)

Yomosa's model for peptide chains is generalized in two respects. (1) The internal vibrations of the peptide groups are incorporated by considering a one-dimensional lattice with alternating masses and alternating linear and nonlinear interactions for the intrapeptide bonds and the hydrogen bonds between the peptide groups, respectively. (2) Discreteness effects are taken into account by applying a new version of Collin's quasicontinuum approach. In the cases in which this approach is not sufficient, we apply an iterative method where the accuracy can be increased systematically. We obtain very narrow solitons with lower and upper velocity limits. Our results have been confirmed by computer simulations. The lifetime of the solitons is finite due to the emission of optical phonons. However, using α -helix parameters, this effect is negligible.

I. INTRODUCTION

For the past 35 years the question of energy transport in muscle proteins has gained considerable attention. The biological energy quantum is given by the hydrolysis of adenosine triphosphate (ATP) as 0.42 eV. It is assumed that this energy is transported practically without loss through the macromolecules and is eventually used for the contraction of muscle fibers. The soliton concept can give an elegant answer to this question because here the dispersion of the energy can be prevented by nonlinear effects.

The fibers of striated muscles in vertebrates contain many myofibrils consisting of sarcomeres. Each sarcomere consists of parallel-running thick and thin filaments. The basic mechanism for muscle contraction consists of sliding the thin filaments relative to the thick ones.¹ This sliding can be described by phenomenological models consisting of a sequence of molecular processes.^{2,3}

The thick filaments consist of myosin molecules, which resemble rods with a diameter of about 40 Å and a length of about 1600 Å. The myosin consists of two polypeptide chains forming a double α -helical structure. At one end there are globular heads where the ATP hydrolysis takes place.

In each helix there are three chains of peptide groups coupled by hydrogen bonds. Beginning in 1973, Davydov⁴ has developed a quantum theory for solitons on these hydrogen-bonded chains. The idea is that the energy from the ATP hydrolysis leads to an excitation of the amide-I vibration in the first peptide groups at one end of the chain. This vibration has an energy of about 0.205 eV and an electric dipole moment of 0.30 debye which is directed approximately along the helix axis. By the dipole-dipole interaction the next peptide groups on the chain can be excited, and so on. However, in this way the energy would not be transported but only dispersed. The essential point in Davydov's assumption is that the vibrational excitations are coupled *nonlinearly* to a deformation of the hydrogen bonds. If the coupling exceeds a certain threshold, solitons can be formed which

are solutions of a nonlinear Schrödinger equation. Further assumptions must be made in order to explain how the solitons eventually produce a relative sliding between thick and thin filaments (see above).

Davydov's model has been refined or modified by several authors, which we do not discuss here because the stability of the solitons now appears to be questionable. Both thermal⁵ and quantum fluctuations⁶ reduce the lifetime such that it may not be large enough for the biological energy transport. (However, for one of the modified models the stability against thermal fluctuations seems to be better.⁷) Moreover, some doubts have appeared recently as to whether the nonlinear Schrödinger equation can be derived properly from Davydov's Hamiltonian.⁸

In 1984 Yomosa⁹ proposed an alternative model that is much simpler than Davydov's model because only the hydrogen bonds are involved in the energy transport. The peptide groups are rigid; i.e., they are represented by single masses which are coupled by strongly *nonlinear* hydrogen bonds. Thus the energy is transported by *lattice solitons*, which has several advantages.

(i) The conditions for the occurrence of solitary waves on a one-dimensional lattice are very weak;¹⁰ this means that every realistic interaction potential can be used, e.g., Lennard-Jones or Morse potentials. Solitons in the mathematical sense exist only for a completely integrable model, the Toda lattice, but for simplicity we will generally use the term soliton.

(ii) Lattice solitons are nontopological; i.e., there is no energy gap. Thus the whole energy of a soliton can be converted into mechanical work for the muscle contraction.⁹ By contrast, Davydov solitons show an energy gap and only the kinetic part of the energy can be converted.

(iii) Using lattice solitons, a molecular interpretation can be given⁹ for the phenomenological "rowing boat" model³ which describes the relative sliding between thick and thin filaments (see above).

(iv) Molecular-dynamics simulations by Perez and Theodorakopoulos¹¹ have shown that lattice solitons are very stable against thermal fluctuations, even at room temperature. Moreover, the lattice solitons are more

stable than Davydov solitons if collisions between the two types of solitons are considered.¹¹

(v) Quantum mechanics is necessary only for the initial condition. The idea is that the energy quantum of 0.42 eV released by the ATP hydrolysis produces impulsively a pulselike compression of the hydrogen-bonded lattice. According to the inverse scattering theory,¹² an arbitrary initial pulse develops into a finite number of solitons plus a radiative background (phonons). This result holds for integrable classical systems. However, at least for one integrable *quantum* lattice model solitonlike excitations have been found: For the quantum Toda lattice in the strong-coupling regime there is a branch of excitations with a dispersion curve (energy vs momentum) which is practically identical to that of the *classical* solitons, though the ground state shows large quantum fluctuations.¹³ In Appendix A we show that a quantum Toda lattice with Yomosa's α -helix parameters⁹ is in fact in the classical regime. Moreover, in the classical *limit* energy and momentum of the solitary excitations are \hbar -free, contrary to the phonons which are semiclassical.^{14,15} For *nonintegrable* lattice models we assume that the situation will be qualitatively similar. In Sec. VII we outline a method to check whether such a model is in the classical regime.

For the above reasons lattice solitons are very good candidates for the energy transport. In this paper we generalize Yomosa's model⁹ in two ways; (i) The peptide groups are no longer rigid. For simplicity we consider only one internal degree of freedom (Sec. II) which leads to interesting new features for the solitons (Sec. IV); the generalization to more degrees of freedom is straightforward (Sec. VII). (ii) Contrary to Yomosa, we do not work in the continuum limit. In fact, discreteness effects turn out to be decisive. These effects are first taken into account by applying the quasicontinuum approach (QCA) of Collins;¹⁶ we use a recent rederivation of the approach in Fourier space¹⁷ which offers several advantages (Sec. III). However, at least for a part of the relevant energy range, the QCA is not sufficient (Sec. V). Therefore we apply an iterative method¹⁷ where the accuracy of taking into account the discreteness effects can be increased as much as necessary (Sec. VI). Finally, we discuss the energy loss of the solitons due to the emission of optical phonons (Section VI). The results of the various sections are always checked by computer experiments.

II. MODEL

Following Yomosa⁹ and Perez and Theodorakopoulos¹¹ we consider a one-dimensional lattice of hydrogen-bonded peptide groups. The nonlinear interactions between neighboring peptide groups are described by a suitable potential V , e.g., a Toda potential or a Lennard-Jones potential, with parameters from the literature (Sec. V).

In contrast to Refs. 9 and 11 we do not neglect the internal vibrations of the peptide groups. As a first approximation we describe each group by two masses M_1 and M_2 coupled by a linear interaction with eigenfre-

quency Ω_0 (Fig. 1). The resulting Lagrangian is

$$L = \sum_n \left[\frac{1}{2} M_1 \dot{A}_n^2 + \frac{1}{2} M_2 \dot{B}_n^2 - V(A_{n+1} - B_n) - \frac{1}{2} m \Omega_0^2 (B_n - A_n)^2 \right], \quad (2.1)$$

where m is the reduced mass; A_n and B_n are displacements from the equilibrium positions.

The neglect of anharmonic terms for the internal vibrations is justified by the fact that the covalent bonds within the peptide groups are considerably stronger than the hydrogen bonds. Thus the relative displacements for the internal motion,

$$\Delta_n = (B_n - A_n)/a, \quad (2.2)$$

are expected to be much smaller than the relative displacements

$$\varphi_n = (A_{n+1} - B_n)/a \quad (2.3)$$

of the hydrogen bonds.

Δ_n and φ_n are defined in units of the equilibrium distance a of neighboring hydrogen bonds, times in units of Ω_0^{-1} , and energies in units of $m \Omega_0^2 a^2$. After this scaling we write the nonlinear interaction in the form $\alpha V(\varphi_n)$ where the harmonic part of V has the form $\frac{1}{2} \varphi_n^2$. The dimensionless parameter α measures the strength of the nonlinear interaction compared to the linear one. In this notation the equations of motion are

$$\ddot{\varphi}_n + \alpha \frac{\delta V}{\delta \varphi_n} - \frac{1}{1+\mu} (\mu \Delta_n + \Delta_{n+1}) = 0, \quad (2.4a)$$

$$\ddot{\Delta}_n + \Delta_n - \frac{\alpha}{1+\mu} \left[\mu \frac{\delta V}{\delta \varphi_n} + \frac{\delta V}{\delta \varphi_{n-1}} \right] = 0, \quad (2.4b)$$

with the mass ratio $\mu = M_1/M_2$.

As Δ_n appears only linearly, it can be eliminated, which leads to a fourth-order equation in time

$$\frac{\partial^2}{\partial t^2} \left[\ddot{\varphi}_n + \varphi_n + \alpha \frac{\delta V}{\delta \varphi_n} \right] + c_m^2 \alpha \left[2 \frac{\delta V}{\delta \varphi_n} - \frac{\delta V}{\delta \varphi_{n+1}} - \frac{\delta V}{\delta \varphi_{n-1}} \right] = 0, \quad (2.5)$$

with

$$c_m^2 = \frac{\mu}{(1+\mu)^2} = \frac{m}{M}, \quad (2.6)$$

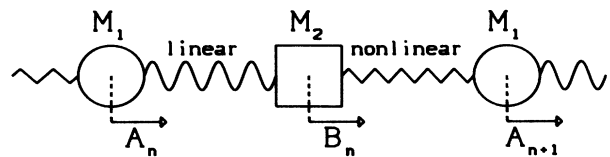


FIG. 1. Peptide chain modeled by a diatomic lattice with alternating linear and nonlinear interactions for the intrapeptide bonds and the hydrogen bonds between the peptide groups, respectively.

where $M = M_1 + M_2$ is the total mass.

Linearization ($\delta V / \delta \varphi_n \simeq \varphi_n$) yields the dispersion curves of acoustic and optical phonons

$$\omega_{\pm}^2(q) = \frac{1+\alpha}{2} \left[1 \pm \left[1 - \frac{16\alpha}{(1+\alpha)^2} c_m^2 \sin^2 \frac{q}{2} \right]^{1/2} \right]. \quad (2.7)$$

The sound velocity is

$$c_s = \left[\frac{\alpha}{1+\alpha} \right]^{1/2} c_m. \quad (2.8)$$

III. QUASICONTINUUM APPROXIMATION

For the diatomic chain with nonlinear nearest-neighbor interactions, a standard decoupling technique in the continuum limit¹⁸ can be used and yields “acoustic” pulse-type solitary waves and “optical” envelope-type solitary excitations.¹⁹ These calculations are rather involved, even more for our model which has not only alternating masses but also alternating interactions.

We prefer not to apply this method because there are two general problems. (i) Only polynomial interaction potentials can be used; usually the realistic potentials are expanded up to the fourth order, assuming that the anharmonicities are small. (ii) In the standard continuum approximation the difference operator is expanded up to a certain order which can lead to an ill-posed Cauchy problem.²⁰ This difficulty occurs because the dispersion due to the discreteness of the system is not taken into account consistently.

For the monoatomic chain both problems have been overcome by the quasicontinuum approximation (QCA) of Collins¹⁶ for solitary waves and periodic modes. Here the difference operator is inverted instead of expanded. Rosenau²⁰ developed a still more general approximation scheme which reduces to the Collins result in the case of solitary waves.

For the diatomic chain, Collins²¹ considered only pulselike solitary waves. We are not interested here in the optical solitons because for the energy transport the pulse solitons are much better candidates. (i) They are supersonic, in contrast to the optical ones. (ii) The mechanism needed for the conversion of the energy into a shortening of muscle fibers seems to be simple only for pulse solitons.⁹

Since the QCA overcomes the above mentioned problems we now apply it to our diatomic model with alternating interactions. However, we use a recent rederivation of the QCA in Fourier space.¹⁷ This formulation is much simpler than the original one¹⁶ and can easily be generalized from the monoatomic chain to our model.

We are interested in solitary waves

$$\varphi_n(t) = \varphi(n - ct) = \varphi(z) \quad (3.1)$$

with velocity c , satisfying the boundary conditions

$$\lim_{|z| \rightarrow \infty} \frac{d^l}{dz^l} \varphi(z) = 0, \quad l = 0, 1, 2, \dots \quad (3.2)$$

Because of these conditions, and analogous ones for $\Delta(z)$,

the Fourier transforms exist,

$$\tilde{\varphi}(q) = \int_{-\infty}^{\infty} dz e^{-iqz} \varphi(z) \quad (3.3)$$

and $\tilde{\Delta}(q)$. Moreover we define the force

$$F(z) = \alpha \frac{\delta V}{\delta \varphi(z)} \quad (3.4)$$

and its Fourier transform $\tilde{F}(q)$.

The equations of motion (2.4) now read

$$-c^2 q^2 \tilde{\varphi} + \tilde{F} - \frac{1}{1+\mu} (e^{iq} + \mu) \tilde{\Delta} = 0, \quad (3.5a)$$

$$(-c^2 q^2 + 1) \tilde{\Delta} - \frac{1}{1+\mu} (e^{-iq} + \mu) \tilde{F} = 0. \quad (3.5b)$$

The elimination of $\tilde{\Delta}$ yields

$$c^2 q^2 (1 - c^2 q^2) \tilde{\varphi}(q) = [4c_m^2 \sin^2(q/2) - c^2 q^2] \tilde{F}(q), \quad (3.6)$$

which can also be obtained directly from (2.5).

According to Ref. 17 the QCA now consists of the following steps. We write (3.6) as

$$A(q) \tilde{\varphi}(q) = \tilde{F}(q) \quad (3.7)$$

and expand $A(q)$ in a Taylor series for $|q| < q_c$, where q_c is the radius of convergence. A truncation after the second term and an inverse Fourier transformation yields a second-order differential equation

$$a_0 \varphi(z) - a_2 \varphi''(z) = F(z), \quad (3.8)$$

which allows the pulselike solutions we are interested in. In fact, (3.8) has the structure which occurred already in the monoatomic case,^{16,17} apart from the coefficients which here have the form

$$a_0 = \frac{c^2}{c_m^2 - c^2}, \quad (3.9)$$

$$a_2 = a_0 \left[\frac{c_m^2}{12(c_m^2 - c^2)} - c^2 \right]. \quad (3.10)$$

Since F is the functional derivative of $V(\varphi(z))$ the integration of (3.8) yields the general result

$$\frac{1}{2} a_2 [\varphi'(z)]^2 + V_{\text{eff}}(\varphi(z)) = 0, \quad (3.11)$$

with

$$V_{\text{eff}} = \alpha V(\varphi) - \frac{1}{2} a_0 \varphi^2, \quad (3.12)$$

where we have set $V(0) = 0$.

Because of $c_m^2 \leq \frac{1}{4}$, a_2 in (3.11) is always positive and can be interpreted as an effective mass. Equation (3.11) has pulselike, solitary solutions if there is a range of φ for which $V_{\text{eff}}(\varphi) \leq 0$, where the equality must hold at the boundaries of this range. For the intermolecular potentials we are considering we have $V_{\text{eff}}(\varphi) \leq 0$ for a negative range $\varphi_1 \leq \varphi \leq 0$, with $a_0 > 0$ and $\alpha < a_0$ (because $V \simeq \varphi^2/2$ for small φ). These conditions lead to

$$c_s < c < c_m, \quad (3.13)$$

which means that we get *supersonic, compressional soli-*

tary waves with amplitude φ_1 . The meaning of the upper limit c_m will be discussed in Sec. IV.

The shape $\varphi(z)$ of the pulses is obtained by the integration of (3.11),

$$z(\varphi) = \int_{\varphi_1}^{\varphi} \frac{d\varphi'}{\pm \sqrt{-2V_{\text{eff}}(\varphi')/a_2}}. \quad (3.14)$$

This integral must be calculated numerically in the case of the Toda or Lennard-Jones potential. However, if we use an expansion of these potentials up to the fourth order,

$$V(\varphi) = \frac{1}{2}(\varphi^2 - 2\beta\varphi^3 + 2\gamma\varphi^4), \quad (3.15)$$

where $9\beta^2 < 16\gamma$, the integral (3.14) can be evaluated analytically and yields in the case of compressional pulses

$$\varphi(z) = \frac{\varphi_1}{1 + [(\varphi_2 - \varphi_1)/\varphi_2] \sinh^2(Qz)}, \quad (3.16)$$

with

$$\varphi_{1/2} = \frac{\beta}{2\gamma} \left[1 \mp \left[1 + 2 \frac{\gamma}{\beta^2} \frac{c^2 - c_s^2}{c_s^2} \frac{c_m^2}{c_m^2 - c^2} \right]^{1/2} \right], \quad (3.17)$$

$$Q^2 = -\varphi_1 \varphi_2 \frac{\gamma \alpha}{2a_2}. \quad (3.18)$$

For the relative motions within the peptide groups we obtain from (3.5a) and (3.6)

$$\bar{\Delta}(q) = \frac{\mu + e^{-iq}}{1 + \mu} \frac{c^2 q^2}{4c_m^2 \sin^2(q/2) - c^2 q^2} \bar{\varphi}(q). \quad (3.19)$$

In order to be consistent with the approximations leading to (3.8), we expand (3.19) to order q^2 and perform an inverse Fourier transformation which yields

$$\Delta(z) = a_0 \left[\varphi(z) - \frac{1}{1 + \mu} \varphi'(z) + \left[\frac{1}{2(1 + \mu)} - \frac{a_0 c_m^2}{12c^2} \right] \varphi''(z) \right]. \quad (3.20)$$

IV. VELOCITY RANGE FOR THE QUASICONTINUUM APPROACH

There are restrictions for the velocity of the solitons, both for technical reasons and in principle. We discuss the latter point first. In (3.7) the function

$$A(q) = \frac{c^2 q^2 (1 - c^2 q^2)}{4c_m^2 \sin^2(q/2) - c^2 q^2} \quad (4.1)$$

has been expanded in a Taylor series which implies that the Fourier transform $\bar{\varphi}(q)$ of the solitary wave must be negligible for $|q| \geq q_c$. Here q_c is the radius of convergence, defined by the first nontrivial solution of

$$2c_m |\sin(q/2)| = cq. \quad (4.2)$$

In Fig. 2 this condition is visualized as the intersection of the straight line cq with the dispersion curve

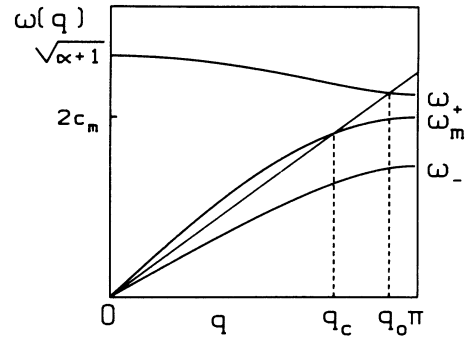


FIG. 2. Phonon dispersion curves. $\omega_+(q)$, optical; $\omega_-(q)$, acoustic; $\omega_m(q)$, monotonic from (4.2). The intersections with the straight line cq (c is the soliton velocity) are discussed in Secs. IV and VI. Parameters: $\alpha=0.6$, $\mu=2$, and $c/c_s=1.3$.

$\omega_m(q) = 2c_m |\sin(q/2)|$. Going back to the original units, ω_m can be identified as the dispersion of a monatomic chain of masses $M = M_1 + M_2$ with a linear interaction with coupling constant $m\Omega_0^2$. For this reason we see now that the upper limit c_m for the soliton velocity in (3.13) results from the linear interaction in our diatomic model with alternating linear and nonlinear interactions. For the usual diatomic model there is no upper limit for the velocity.²¹

In practice, i.e., for solitons with a finite width, the condition (3.13) even must be tightened to

$$c_s < c \ll c_m; \quad (4.3)$$

otherwise q_c is very small and the Fourier transform $\bar{\varphi}(q)$ cannot be negligible for $|q| \geq q_c$.

Moreover, the lower limit c_s leads to a further restriction. The sound velocity

$$c_s = [\alpha/(1 + \alpha)]^{1/2} c_m \quad (4.4)$$

is the slope of the acoustic branch $\omega_-(q)$ for $q \rightarrow 0$ (Fig. 2). In order to ensure a certain range of soliton velocities satisfying both conditions in (4.3), we must demand $\alpha \ll 1$. In fact, this is fulfilled for our model since the hydrogen bonds between the peptide groups are considerably weaker than the covalent bonds within these groups (α is the ratio of the coupling strengths, see Sec. II). In Sec. V we will give estimates for α .

So far we have discussed only the limitations which result from the finite radius of convergence for the Taylor series of $A(q)$. Moreover we must test whether the truncation (3.8) behind the second term of the series is justified. For a given mass ratio μ , i.e., for given c_m , we choose a velocity c satisfying (4.3) and estimate the q range for which the truncated expansion agrees well with $A(q)$. Then we choose a potential V and calculate the solitary wave $\varphi(z)$ which belongs to c . Its Fourier transform $\bar{\varphi}(q)$ must be negligible outside of the above mentioned q range. The results of this test are given in Sec. V.

V. SOLITARY WAVES FOR REALISTIC PARAMETER VALUES

The lattice constant a for the H-bonded peptide chains in the α helix is about 4.5 \AA .⁹ For the eigenfrequencies of a peptide group we choose as a representative value $\Omega_0 = 3.11 \times 10^{14} \text{ sec}^{-1}$ from the amide-I vibration. The total mass $M = M_1 + M_2$ corresponds to the mass of a peptide group plus an average residue in a muscle protein, which gives together about 100 proton masses.^{9,11} The mass ratio $\mu = M_1/M_2$ is kept as a free parameter which is varied between 1 and 10 (our results are invariant under the transformation $\mu \rightarrow 1/\mu$).

We model the hydrogen bonds between neighboring peptide groups by a suitable nonlinear interaction, e.g., a Toda potential with parameters fitted to an *ab initio* self-consistent-field molecular-orbital (SCF MO) calculation for a H bond in a formamide dimer.⁹ In our dimensionless units this corresponds to

$$\alpha V_T(\varphi) = \frac{\alpha}{\beta^2} [\exp(-\beta\varphi) + \beta\varphi - 1], \quad (5.1)$$

with $\beta = 18$ and $\alpha = 0.00123/c_m^2$. (Note that in Sec. III the interaction was introduced in the form αV , where $V = \varphi^2/2$ for $\varphi \rightarrow 0$.) With these parameters the sound velocity is $c_s \approx 4900 \text{ m/sec}$ for $1 \leq \mu \leq 10$.

As a second example we take a Lennard-Jones potential with parameters fitted to the equilibrium distance a and the bond energy,^{11,22} which gives

$$V_{LJ}(\varphi) = \frac{1}{72} \left[\frac{1}{(1+\varphi)^{12}} - \frac{2}{(1+\varphi)^6} + 1 \right] \quad (5.2)$$

and $\alpha = 0.000811/c_m^2$. The corresponding sound velocity is about 4000 m/sec for $1 \leq \mu \leq 10$.

For fixed mass ratio μ , i.e., for fixed c_m , we choose a velocity c from the range (4.3) and calculate the corresponding solitary wave $\varphi(z)$ by (3.14), and its Fourier transform $\tilde{\varphi}(q)$. A first test shows (Fig. 3) that $\tilde{\varphi}(q_c)/\tilde{\varphi}(0)$ is indeed negligible for a large range of veloc-

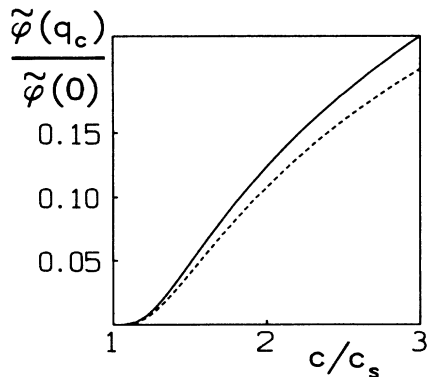


FIG. 3. Fourier transform $\tilde{\varphi}$ of the QCA solution at the radius of convergence q_c of the Taylor series of (4.1) as a function of the soliton velocity c . Toda and Lennard-Jones potentials from Sec. V (solid and dashed line, respectively), with $\mu = 1$.

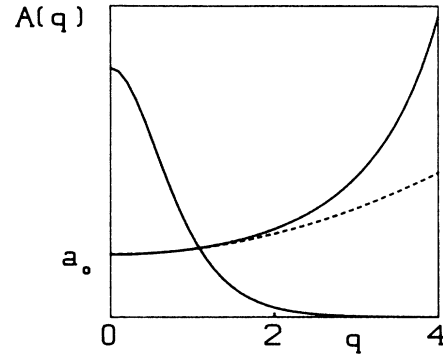


FIG. 4. $A(q)$ from (3.7) and its truncated Taylor expansion (solid and dashed line, respectively), for $\mu = 1$ and $c/c_s = 1.05$. For comparison $\tilde{\varphi}(q)$ using a Toda potential is shown.

ities (about 30% above c_s) as expected from the discussion of the radius of convergence q_c in Sec. IV.

However, this large velocity range is considerably reduced by the second test described in Sec. IV. For the potentials and parameter values used here, the QCA is valid for velocities c which do not exceed the sound velocity by more than about 5–10%; Fig. 4 shows an example for $c = 1.05c_s$.

Eventually we perform a final test by comparing with a computer simulation: We take (3.14) and (3.20) as initial conditions and integrate the difference-differential equations (2.4) numerically (see Appendix B). The time evolution of a single pulse (Fig. 5) shows that the QCA solution is a good approximation: Only very small oscillations (phonons) appear immediately after the start; after a while these phonons are left behind and the pulse travels without changing its shape (see Sec. VI, however). Figure 6 shows the scattering of two solitons.

After these tests we turn to the essential question whether the solitons of the QCA can transport enough energy. Figure 7 shows the energy E of a single soliton as a function of c/c_s (for both our potentials). E must be compared with the biological energy quantum of 0.42 eV (see the introduction). Yomosa⁹ assumed that these quanta set the initial conditions for the lattice solitons. Naturally, an arbitrary initial condition generally pro-

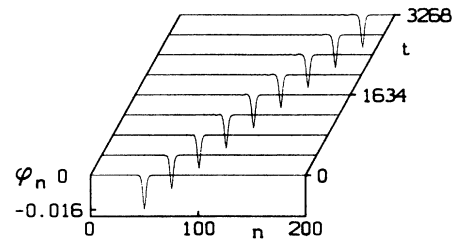


FIG. 5. Computer simulation for a chain of 200 unit cells, using a QCA soliton with $c/c_s = 1.05$ as initial condition, a Toda potential, and $\mu = 1$.

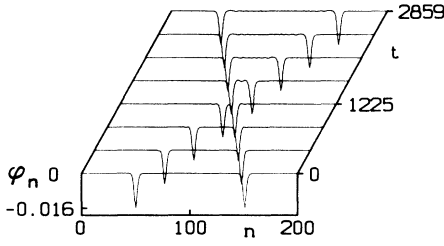


FIG. 6. Collision of two QCA solitons, same parameters as in Fig. 5.

duces several solitons plus an oscillatory background. Knowing that nature usually works fairly effectively, and in order to be on the safe side, let us assume that the energy of one quantum essentially goes into one or two solitons. Then we see from Fig. 7 that we need a velocity of at least $1.2c_s$, for which the QCA clearly is no longer valid. Naturally, this velocity is only a rough estimate that depends on the energy unit $m\Omega_0^2 a^2$, i.e., on our choice of Ω_0 . But in any case we need a new method in order to handle the case of larger velocities, and this is presented in Sec. VI.

VI. ITERATIVE METHOD AND STABILITY

With increasing velocity and energy the solitary waves become narrower, their width can be in the order of the lattice constant. In this case the QCA can no longer work. It also would not help to take more terms of the Taylor expansion of $A(q)$ in (3.7); the resulting higher-order differential equations cannot be integrated like (3.8). Moreover, even the infinite Taylor series cannot fully represent $A(q)$ because of the finite radius of convergence.

Recently for the monatomic chain an *iterative* method¹⁷ has been developed. Here the accuracy of taking into account the discreteness effects is increased systematically. In the case of the Toda lattice the iteration converges to the exact one-soliton solution.

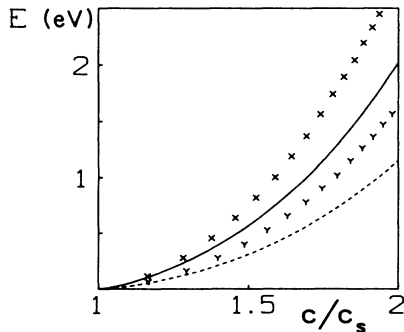


FIG. 7. Soliton energy vs velocity c , using Toda interactions (solid line, QCA result; x , iterative solution) or Lennard-Jones interactions (dashed line, QCA; y , iterative solution).

This method can also be applied to the pulse-type solitary waves of our diatomic model: Our basic equation (3.6) can be written in the form

$$\bar{\varphi}(q) = A^{-1}(q)\bar{F}(q), \quad (6.1)$$

which already suggests an iteration because $\bar{F}(q)$ is the Fourier transform of $F(\varphi(z))$, see (3.4). However, instead of (6.1) we use a slightly different form which will turn out later to be more convenient: We first split off the linear part of the force (3.4) and denote the nonlinear part by G

$$F(\varphi(z)) = \alpha[\varphi(z) + G(\varphi(z))]. \quad (6.2)$$

Inserting (6.2) into (3.6) and isolating $\bar{\varphi}$ we get

$$\bar{\varphi}(q) = \frac{\alpha[c^2 q^2 - \omega_m^2(q)]}{[c^2 q^2 - \omega_+^2(q)][c^2 q^2 - \omega_-^2(q)]} \bar{G}(q), \quad (6.3)$$

where $\omega_{\pm}(q)$ and $\omega_m(q)$ are the dispersion curves (2.7) and (4.2), respectively.

Similar to the monatomic case,¹⁷ an iteration for (6.3) would converge only to the trivial solution $\varphi(z) \equiv 0$. This can be prevented by keeping $\bar{\varphi}(0)$ constant during the iteration.¹⁷ This condition leads to the elimination of c from (6.3), and thus to a new iteration procedure

$$\bar{\varphi}_{i+1}(q) = \frac{\alpha[c_i^2 q^2 - \omega_m^2(q)]}{[c_i^2 q^2 - \omega_+^2(q)][c_i^2 q^2 - \omega_-^2(q)]} \bar{G}_i(q), \quad (6.4)$$

with

$$c_i^2 = c_s^2 \frac{\bar{\varphi}_i(0) + \bar{G}_i(0)}{\bar{\varphi}_i(0) + c_s^2/c_m^2 \bar{G}_i(0)}. \quad (6.5)$$

This implies $c_s < c_i < c_m$, i.e., the same condition as for the QCA, cf. (3.13).

Each iteration consists of 4 steps:

$$G_i(z) = G(\varphi_i(z)),$$

$\bar{G}_i(q)$ by Fourier transformation,

calculation of $\bar{\varphi}_{i+1}(q)$ by (6.4),

$\varphi_{i+1}(z)$ by inverse Fourier transformation.

As starting function $\varphi_1(z)$ we choose the QCA result.

The elimination of c from (6.3) means that the iteration process does not select a solution with a given velocity c , but a solution with a given integrated amplitude

$$\bar{\varphi}_1(0) = \int_{-\infty}^{\infty} dz \varphi_1(z). \quad (6.6)$$

c_i changes during the iteration and converges towards a value which usually is considerably lower than the initial one (Fig. 8). By the way, this behavior is qualitatively similar to that during a computer simulation: Starting with an approximate solution as initial condition, an adaptation to the lattice by the emission of phonons is observed. The resulting solitary wave has a lower velocity (and energy) than the initial wave.

For the potentials and parameters used here, a *sufficient* convergence is achieved after at most eight

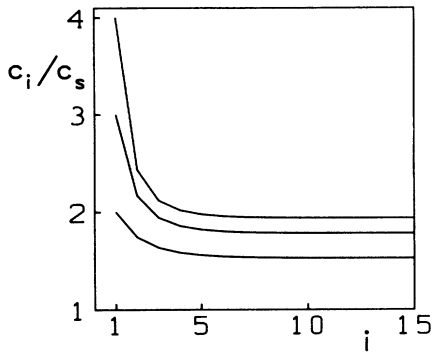


FIG. 8. Velocities c_i from (6.5) during the iteration, for 3 initial velocities $c_1=4c_s, 3c_s, 2c_s$; using a Toda potential and $\mu=1$.

iterations. As a test, the results were used as input for a computer simulation. Contrary to the QCA result for a velocity outside of the validity range [Fig. 9(a)], the shape of the pulse remains unchanged, no adaption to the lattice is observed [Fig. 9(b)]. The soliton character of the pulses is also seen clearly in scattering experiments, even in the highly discrete regime (Fig. 10). Figure 7 shows the soliton energies; they are considerably higher than the QCA results for the same velocities.

However, a *complete* convergence cannot be achieved, i.e., an exact solitary wave solution probably does not exist. In fact, contrary to the monatomic case,¹⁷ our iteration procedure (6.4) shows a pole, namely, at the solution q_0 of

$$c_i q = \omega_+(q). \quad (6.7)$$

The existence of the pole means that (6.4) makes sense only if $\tilde{G}(q)$ and $\tilde{\varphi}(q)$ are negligible for $|q| \geq q_0$. In practice a cutoff is necessary in each step of the iteration, see Appendix B.

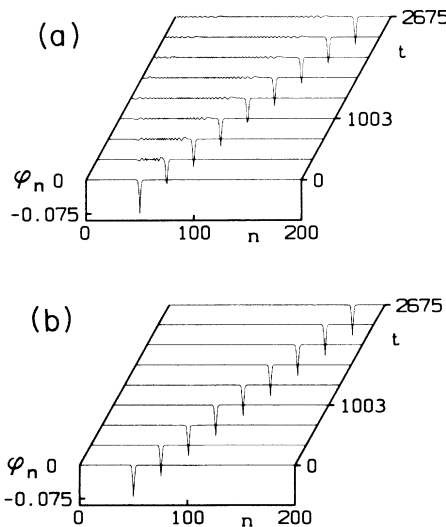


FIG. 9. Computer experiments with solutions for $c/c_s=1.28$. (a) QCA result; (b) iterative solution as initial condition, using a Toda potential and $\mu=1$.

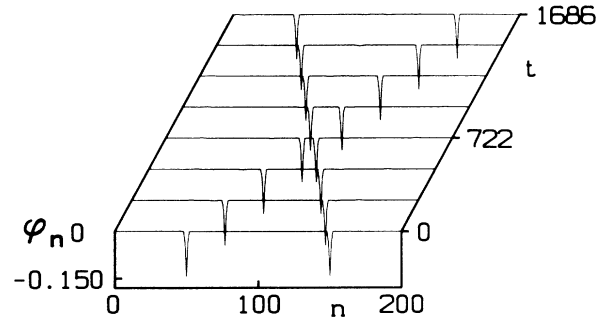


FIG. 10. Collision experiment, using as initial data two very narrow solitons (with $c/c_s=1.9$) from the iterative solution; for a Toda potential and $\mu=1$.

Contrary to the finite convergence radius q_c which limits the validity range of the QCA (Sec. IV), the occurrence of the pole is not a technical problem but is connected with a physical effect. Peyrard *et al.*²³ showed by computer simulations and theoretical investigations that a solitary wave with velocity c cannot be stable if the line cq has an intersection with one of the phonon branches $\omega(q)$. The solitary wave permanently loses energy by the emission of phonons, their frequency spectrum is centered around $\omega(q_0)$, where q_0 is the intersection point. Due to the energy loss the velocity c decreases gradually, and the width of the wave increases. Thus the discreteness effects which are responsible for the phonon emission become smaller and smaller. Eventually the solitary wave is practically stable because the energy loss is negligible.

This scenario appears for our model, too. The condition (6.7) corresponds to the intersection of $c_i q$ with the optical-phonon branch (Fig. 2). In a computer simulation two very different time scales appear: Starting with any initial condition, including the QCA result, the above-mentioned adaptation to the lattice needs only a rather short time [Fig. 9(a)], this adaptation is not necessary when the result from our iterative method is used as initial condition [Fig. 9(b)]. Contrary to the adaptation process, the emission of optical phonons occurs for a much longer time, in principle it goes on forever while the solitary wave disappears asymptotically.

However, this effect is extremely small when α -helix parameters are used. For example, in Fig. 9(b) no phonon emission is seen. The situation can be illustrated by drawing Fig. 2 using these parameters: As α is very small (Sec. V) there is a wide gap between the acoustic- and optical-phonon branches, and the intersection point q_0 is far outside of the first Brillouin zone (e.g., $q_0 \approx 5\pi$ for $c \approx 2c_s$). Therefore the above condition for the convergence of the iteration [negligible $\tilde{\varphi}(q_0)$ and $\tilde{G}(q_0)$] is indeed very well fulfilled. We conclude that the energy loss due to the emission of optical phonons is negligible in the case of the α helix.

VII. CONCLUSION

Lattice solitons remain good candidates for the energy transport in the α helix when an internal vibration mode

of the peptide groups is taken into account. Our theory can easily be generalized for a lattice with a basis of more than two atoms; e.g., three masses representing a peptide group $N-C=O$. The essential point, which allows the elimination of coordinates in the equations of motion, is the neglect of anharmonicities for the internal vibrations. This neglect is justified because the covalent bonds within the peptide groups are considerably stronger than the hydrogen bonds between the peptides.

Discreteness effects are very important. They are partially incorporated by the quasicontinuum approximation. However, for the parameters of the α helix, a systematic implementation of the discreteness is necessary, which is achieved by an iterative method. The convergence of this method is limited in principle by an instability of the solitons due to the emission of optical phonons. However, this effect turns out to be negligible.

As molecular dynamics simulations have shown that solitons on monatomic lattices are stable against thermal fluctuations,¹¹ we expect that the same will hold for our diatomic lattice.

In our opinion, there are two points which should be settled next.

(1) We must check whether our model is indeed in the classical regime. Contrary to the test for the Toda lattice, for which the quantum version can be treated exactly by the Bethe ansatz (see introduction), our model is not integrable. Nevertheless, an estimate can be given: The canonical momentum p of a soliton can be calculated by two different methods.²⁴⁻²⁶ If the de Broglie wavelength $\lambda = h/p$ turns out to be much smaller than the width of the soliton, we are in the classical regime. (This estimate is equivalent to the use of the uncertainty relation in Appendix A.)

(2) Models are necessary which describe in detail how the energy released by the ATP hydrolysis can be converted into a compressional pulse, serving as initial condition for lattice solitons.

ACKNOWLEDGMENTS

We thank N. Flytzanis, University of Crete, for several valuable discussions concerning the continuum approximation for the diatomic chain.¹⁹ The work of D. H. was supported by Deutsche Forschungsgemeinschaft (DFG), Project No. D 7 of SFB 213.

APPENDIX A

For the monatomic quantum Toda lattice with the interaction

$$V(\varphi) = \frac{m\omega^2}{\gamma^2} [\exp(-\gamma\varphi) + \gamma\varphi - 1] \quad (\text{A1})$$

a dimensionless coupling parameter

$$C = \frac{m\omega}{\hbar\gamma^2} \quad (\text{A2})$$

can be defined.¹⁵ The strong coupling regime $C \gg 1$ is equivalent to the classical regime $E_{\text{sol}} \gg E_{\text{ph}}$, where $E_{\text{sol}} = m\omega^2/\gamma^2$ and $E_{\text{ph}} = \hbar\omega$ are typical soliton and phonon energies, respectively. In practice, already for $C \gtrsim 5$ the dispersion curve for the supersonic excitations cannot be distinguished from that of the classical solitons.

The classical regime can also be obtained from an uncertainty relation. The position of a soliton can be determined within about a lattice constant a , the canonical momentum¹⁵ of a soliton is in the order of $m\omega/(\gamma^2 a)$, which yields again $C \gg 1$.

Yomosa⁹ modeled the hydrogen bonds of the α helix by a Toda potential with the parameters $\gamma = 4 \text{ \AA}^{-1}$ and $m\omega^2/\gamma = 0.31 \text{ eV \AA}^{-1}$. With m being on the order of 100 proton masses we get $m\omega^2/\gamma^2 = 0.08 \text{ eV}$ and $\hbar\omega = 0.0073 \text{ eV}$; thus $C \approx 11$, which is clearly in the classical regime.

APPENDIX B

Two numerical procedures are used in this work. The first is a computer simulation, i.e., the solution of the equations of motion (2.4) for a chain of 401 particles (200 lattice constants, free boundaries) for a given initial condition. Here a fourth-order Runge-Kutta scheme with automatic step-size control is used. The time step is chosen such that the energy of the chain is conserved within a relative accuracy of 10^{-6} . During the simulation, time and length are scaled such that both the velocity of sound c_s and the absolute value of the maximal φ_n are equal to 1.

The second procedure is the iteration (6.4). Here the Fourier transformations are performed as described in Ref. 17. Because of the pole in (6.4) at q_0 defined by (6.7), a cutoff is necessary for $\tilde{\varphi}_{i+1}(q)$. A sharp cutoff would induce oscillatory tails in $\varphi_{i+1}(z)$, which are unwelcome since we expect a pulselike form. Therefore we replace $\tilde{\varphi}_{i+1}(q)$ for $|q| \geq q_1$ by an exponential decaying function; here q_1 must be chosen such that $\tilde{\varphi}_{i+1}(q_1) \ll \tilde{\varphi}_{i+1}(0)$. In practice we take one of the grid points close to the first zero of $\tilde{\varphi}_{i+1}(q)$.

¹H. E. Huxley and J. Hanson, *Nature* **173**, 973 (1954); *Structure and Function of Muscle* (Academic, New York, 1960), p. 183; A. F. Huxley and R. Niedergerke, *Nature* **173**, 971 (1954); A. F. Huxley, *Proc. Biophys.* **7**, 255 (1957).

²A. F. Huxley and A. Simmons, *Nature* **233**, 533 (1971).

³J. M. Murray and A. Weber, *Sci. Am.* **230**, 1974 (1974).

⁴A. S. Davydov, *J. Theor. Biol.* **38**, 559 (1973); *Stud. Biophys.* **47**, 221 (1974); *Phys. Scr.* **20**, 387 (1979); *Biology and Quantum Mechanics* (Pergamon, New York, 1982).

⁵P. S. Lomdahl and W. C. Kerr, *Phys. Rev. Lett.* **55**, 1235 (1985); A. F. Lawrence, J. C. McDaniel, D. B. Chang, B. M. Pierce, and R. R. Birge, *Phys. Rev. A* **33**, 1188 (1986).

- ⁶H. Bolterauer and M. Opper (unpublished).
- ⁷L. Cruzeiro, J. Halding, P. L. Christiansen, O. Skovgaard, and A. C. Scott, *Phys. Rev. A* **37**, 880 (1988).
- ⁸D. W. Brown, K. Lindenberg, and B. J. West, *Phys. Rev. A* **33**, 4104 (1986); D. W. Brown, B. J. West, and K. Lindenberg, *Phys. Rev. A* **33**, 4110 (1986).
- ⁹S. Yomosa, *J. Phys. Soc. Jpn.* **53**, 3692 (1984); *Phys. Rev. A* **32**, 1752 (1985).
- ¹⁰M. K. Ali and R. L. Somorjai, *J. Phys. A* **12**, 2291 (1979); J. R. Rolfe, S. A. Rice, and J. Dancz, *J. Chem. Phys.* **70**, 26 (1979); M. A. Collins, *Chem. Phys. Lett.* **77**, 342 (1981); H. Bolterauer, in *Recent Developments in Condensed Matter Physics*, edited by J. T. Devreese, L. F. Lemmens, and V. E. van Doren (Plenum, New York, 1981), Vol. 4, p. 199.
- ¹¹P. Perez and N. Theodorakopoulos, *Phys. Lett. A* **117**, 405 (1986); **124**, 267 (1987).
- ¹²C. S. Gardner, J. M. Greene, M. D. Kruskal, and R. M. Miura, *Phys. Rev. Lett.* **19**, 1095 (1967).
- ¹³F. G. Mertens and M. Hader, in *Dynamical Problems in Soliton Systems*, Vol. 30 of *Springer Series in Synergetics*, edited by S. Takeno (Springer, Berlin, 1985), p. 89.
- ¹⁴B. Sutherland, *Rocky Mount. J. Math.* **8**, 413 (1978).
- ¹⁵F. G. Mertens, *Z. Phys. B* **55**, 353 (1984).
- ¹⁶M. A. Collins, *Chem. Phys. Lett.* **77**, 342 (1981); M. A. Collins and S. A. Rice, *J. Chem. Phys.* **77**, 2607 (1982).
- ¹⁷D. Hochstrasser, F. G. Mertens, and H. Büttner, *Physica D* **35**, 259 (1989).
- ¹⁸H. Büttner and H. Bilz, in *Solitons in Condensed Matter Physics*, edited by A. R. Bishop and T. Schneider (Springer, Berlin, 1978), p. 162.
- ¹⁹St. Pnevmatikos, M. Remoissenet, and N. Flytzanis, *J. Phys. C* **16**, L305 (1983); St. Pnevmatikos, N. Flytzanis, and M. Remoissenet, *Phys. Rev. B* **33**, 2309 (1986).
- ²⁰P. Rosenau, *Phys. Lett. A* **118**, 222 (1986); *Phys. Rev. B* **36**, 5868 (1987).
- ²¹M. A. Collins, *Phys. Rev. A* **31**, 1754 (1985).
- ²²M. Levitt, *J. Mol. Biol.* **168**, 595 (1983).
- ²³M. Peyrard, St. Pnevmatikos, and N. Flytzanis, *Physica* **19D**, 268 (1986).
- ²⁴F. G. Mertens and H. Büttner, *Phys. Lett.* **84A**, 335 (1981).
- ²⁵H. Bolterauer and M. Opper, *Z. Phys. B* **42**, 155 (1981).
- ²⁶N. Flytzanis, St. Pnevmatikos, and M. Peyrard, *J. Phys. A* **22**, 783 (1989).